# ANALYSIS OF HIGH-TEMPERATURE HEAT PUMP AND SEASONAL THERMAL STORAGE INTEGRATION INTO DISTRICT HEATING NETWORKS

Christian Pressa[1*], Verena Jetzinger[1],
Hendric Popma[1], and Matthias Finkenrath[1]

[1]Kempten University of Applied Sciences, Kempten, Germany

*Corresponding Author: christian.pressa@hs-kempten.de

## ABSTRACT

Decarbonization of District Heating and Cooling (DHC) networks has become a priority for network operators. This paper presents the first results of the HeatSHIFT research project, which aims at analyzing benefits of using high-temperature heat pumps within existing district heating networks, particularly those with supply temperatures above 120 °C.
To convert existing DHC infrastructure into more energy-efficient networks that operate at lower temperatures often takes decades and requires significant investments. Using high-temperature heat pumps that are running on renewable electricity for heat generation instead is therefore an interesting decarbonization alternative for operators, particularly in the short or medium term. Apart from reducing $CO_2$ emissions, this also helps to increase the security of heat supply by reducing dependency on – often imported – fossil fuels. The three-year research project HeatSHIFT, funded by the German Federal Ministry for Economic Affairs and Climate Action (BMWK), is focusing on a techno-economic evaluation and optimization of high-temperature heat pump integration into district heating networks. Various heat sources and different high-temperature heat pump technologies are being evaluated. Furthermore, options for combining heat pumps with thermal energy storage are included in the study. In this context, the use of seasonal heat storage is of particular interest, since this makes it possible to transfer large amounts of surplus heat from the summer, typically generated in waste incineration plants, to the winter season. Therefore, use of fossil-fueled peaking units for heat generation can be reduced.
Process simulation is used for modeling and analyzing all key technologies, such as high-temperature heat pumps, thermal energy storages, the DHC network, and power plants. Since the project is supported by district heating system operators, high-temperature heat pump manufacturers and the German industry association for district heating and cooling (AGFW), simulation models can be validated using machine and operating data provided by these partners. In addition, the economic attractiveness of integrating high-temperature heat pumps into DHC networks is evaluated by mixed-integer linear programming, including fluctuations of prices over time on energy markets.

## 1 BACKGROUND

Half of Europe's entire energy consumption is used for heating and cooling, with 75 % derived from fossil sources. Thus, it is important to provide heat as efficiently as possible, also producing the lowest possible greenhouse gas emissions. The legislator in Germany requires operators of heating networks to feed in 30 % based on renewable energies or unavoidable waste heat by 2030, and 80 % by 2040 (Federal Ministry for Economic Affairs and Climate Action 2024). In 2022, the share of renewable energies in district heating was 17 % (Nickel, 2023).
Large heat pumps have the potential to cover up to 70 % of the district heating supply in Germany by 2045, which would make a significant contribution to decarbonization (Ahrendts et al., 2023). District heating suppliers generate high heat surpluses in summer, especially because of the continuous operation of waste-to-energy plants, due to the continual generation of waste, independent of the season. In winter, fossil-fueled peak load boilers are commonly used to provide additional heat during periods


https://doi.org/10.52202/077185-0089

of cold ambient temperatures. Seasonal thermal energy storage systems have the potential to rectify this misalignment between heat generation and heat usage on a seasonal level (Bolton et al., 2023).

## 2 PROJECT OBJECTIVES

The project aims to explore a variety of innovative key technologies and their combinations, focusing specifically on high-temperature heat pumps, different seasonal thermal energy storage technologies and their integration in first-, second- and third-generation district heating systems, which currently dominate the district heating landscape (Connolly et al., 2014). By utilizing process simulation techniques, the HeatSHIFT project models key components and analyzes their potential benefits for district heating networks. Close collaboration with stakeholders, including district heating system operators, heat pump manufacturers and an industry association, ensures the validation of simulation models and incorporates real-world data and insights. This paper includes an economic analysis using mixed-integer optimization, which enables an evaluation of the economic attractiveness of integrating the mentioned technologies into existing DHC networks. Market dynamics, such as fluctuations in energy prices over time, are considered in order to evaluate the financial feasibility.

## 3 DHC NETWORK AND THERMAL GENERATION UNITS

One of the HeatSHIFT project partners is ZAK Energie GmbH, which operates the district heating grid for the city of Kempten and multiple thermal generation units, namely a waste incineration plant and a wood-fired power plant, which is, however, utilized as a second furnace line of the waste incineration plant. Together, these facilities produce electricity for around 20,400 households and heat for approximately 17,770 households. Additionally, a peak load facility with a capacity of 45 $MW_{th}$ ensures heat supply during winter months. A short-term heat storage provides flexibility in peak load scenarios, resulting in an annual coverage of around 3,000 MWh.

Heat load and generation data of high quality were provided to the project by the operator. During summer, a surplus heat of approximately 70 to 80 GWh arises due to the low heat demand from consumers in the district heating network. However, in winter months, there is a heat deficit ranging from 10 to 18 GWh, which is covered by the peak load heating plant. Supply temperatures range from 100 °C to 130 °C depending on the season, with a mean value of 120 °C. Return temperatures are stable in the winter months, ranging between 50 °C and 60 °C, but can get as high as 97 °C during summer months.

## 4 LARGE-SCALE HIGH TEMPERATURE HEAT PUMPS

The term “large-scale” or “industrial” high-temperature heat pump typically refers to those with a heating capacity of 500 kW or more and a sink temperature of 100 °C or higher (Arpagaus et al., 2018). These can be used to provide heat to heating networks, if there is an appropriate heat source available, such as waste heat from an industrial process, an energy storage, or river water (Ahrendts et al., 2023; Pelda et al., 2020).

In heat pumps, the heat transferred between the heat source and the working fluid at low pressure, and between the working fluid at high pressure and the heat sink, can be either sensible or latent heat (Dehli et al., 2023). Whether the heat transferred is sensible or latent depends on the specific cycle and design of the heat pump, which impacts the performance at different temperature levels, as described in the following chapters 4.1 and 4.2 (Längauer, 2021). In this work, two main heat pump operating principles are considered: a conventional heat pump (CHP), based on vapor compression (reverse Rankine cycle), and an innovative heat pump based on a reverse Joule/Brayton cycle. For the Joule/Brayton cycle, the concept of a rotation heat pump (RHP) is analyzed based on operating data provided by the vendor. Both models for the CHP and the RHP were implemented in the software package EBSILON Professional, which is used as a process simulation environment in this project.



https://doi.org/10.52202/077185-0089

### 4.1 Conventional Heat Pump

Conventional heat pump (CHP) technology, based on the reverse Rankine cycle, is used as a baseline process. Since the process efficiency is highly dependent on the components used, their cycle design and the used refrigerant, this project aims at depicting and simulating various possible configurations in combination with different refrigerants. With Siemens Energy as an associated project partner, a special focus is placed on company-related components and refrigerants for large-scale applications.

The particular CHP described in this paper is characterized by a two-stage compression performed by two turbo-compressors and vapor-injection achieved by a flash box, as shown in Figure 1. Technology Collaboration Programme on Heat Pumping Technologies by IEA, 2022 suggests R1233zd as a refrigerant, which is also used for the following simulations in this paper. According to Arpagaus et al., 2018 this refrigerant also provides a possible operating temperature range that matches the investigated heat source and sink temperatures well. Said temperatures are examined for a range from 35 to 80 °C with a temperature decrease of 10 K for the heat source and from 120 to 140 °C for the heat sink with variable temperature lifts. Another investigation of a CHP with very similar properties is also presented in Jiang et al., 2021. Part-load operation can be realized by using bypasses, a speed-controlled drive, or volume flow control, as Technology Collaboration Programme on Heat Pumping Technologies by IEA, 2022 suggests. In the simulation model, a modified efficiency characteristic for the compression is used to consider part-load effects. For this specific use case, a combination of volume flow control for high utilization levels of the heat pump and bypass operation for low utilization levels is assumed. The change in heat transfer efficiency due to partial load operation is taken into account by dimensioning the heat exchanger parameters according to nominal load and using this parametrization for the following calculation of heat transfer in part-load. The modelled CHP shows a high accuracy regarding process efficiency in comparison to validation data provided by Siemens Energy with a maximum relative deviation of 1.37 % for the investigated operating points.

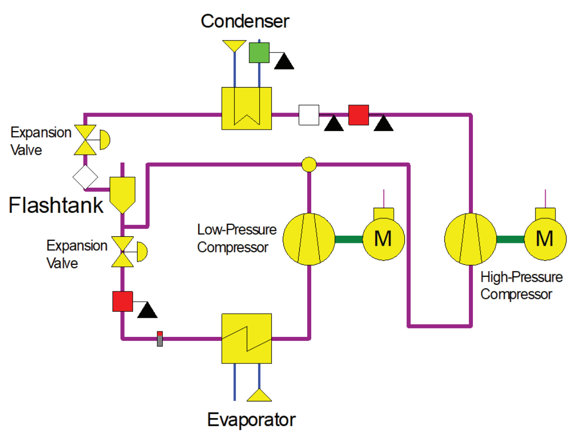


**Figure 1:** Schematics of the conventional heat pump model

### 4.2 Rotation Heat Pumps

The rotation heat pump (RHP) presents new possibilities for heat pump applications, especially in situations where conventional compression heat pumps may not be economically viable. This chapter briefly discusses the fundamental aspects of the underlying process and derives the resulting potential advantages for its application in the HeatSHIFT project. Längauer and Adler and Längauer et al., 2019 offer more in-depth details about the process and the technical implementation. The RHP, based on the reverse Joule/Brayton process, operates on the principle of rotary gas compression, using centrifugal forces.

The heat exchangers are positioned closer (low-temperature heat exchanger) and farther (high-temperature heat exchanger) away from the axis of rotation in a closed cycle. The centrifugal force increases at greater distance from the axis of rotation and thereby the compression of the working gas. According to the developers, the compression and expansion can be achieved with more than 99 % efficiency. The working medium, a noble gas mixture, remains in a gaseous state, which facilitates a sensitive heat transfer of thermal power from both the heat source and the heat sink. Längauer highlights


https://doi.org/10.52202/077185-0089

that a temperature glide in the heat transfer medium and working fluid proves advantageous, resulting in lower exergy losses compared to a temperature profile involving a phase-change medium. This characteristic, coupled with highly efficient compression, is the primary factor contributing to the RHP's claimed elevated Coefficient of Performance (COP) at larger temperature differences, compared to conventional heat pumps (CHP).
The RHP can technically and economically achieve temperatures on the sink side of up to 150 °C. In applications with fluctuating temperatures of the heat source and/or sink, for example due to seasonal variations, the RHP could operate with high efficiency, since operating pressures of the gaseous working fluid can be adjusted accordingly, without being affected by phase changes. In practice, the described process has successfully operated within a temperature range of -20 °C to 150 °C (Längauer, 2021). Despite its promising advantages, the primary challenges in implementing the RHP lie in ensuring efficient compression and managing the system's complex control. The main energy consumer in this process is the fan (Figure 2), which compensates the pressure losses due to pipe friction. In comparison, the energy needed by the rotation drive to establish the rotation-based compression and expansion, is negligible.

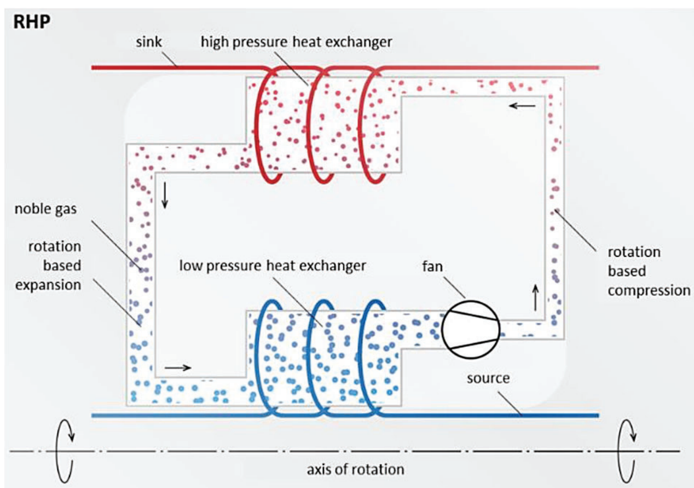


**Figure 2:** Rotation heat pump – basic principle (Längauer and Adler)

## 5 SEASONAL THERMAL ENERGY STORAGE

In district heating networks, the consideration of thermal storage is crucial. The storage of heat becomes relevant when the temporal supply or generation does not align with the demand. Large seasonal thermal energy storages are designed to store heat produced by renewable sources or unavoidable waste heat generated in the summer months for use in the winter months. The most common types include water storages (tank thermal energy storages, pit thermal energy storages) and ground-coupled storages (borehole thermal energy storages, aquifer thermal energy storages). The HeatSHIFT project initially focuses on borehole thermal energy storages (BTES), as this, along with ATES (Aquifer Thermal Energy Storage), is among the most cost-effective storage solutions due to not needing to manufacture a specific storage medium. In contrast to ATES, BTES is not bound to the presence of an aquifer (water-bearing underground layer). Additionally, high-temperature BTES is associated with lower geological risks and can be seamlessly integrated, particularly in densely populated cities (Fleuchaus, 2020; Hirvijoki and Hirvonen, 2022).

### 5.1 Borehole Thermal Energy Storage (BTES)

Borehole Thermal Energy Storage Systems utilize multiple heat exchangers embedded vertically in boreholes in the ground. Boreholes up to 200 meters deep are considered "Medium-Deep" Borehole Thermal Energy Storage (Welsch et al., 2016). The subsurface heat transfer is facilitated by a circulating working fluid within the closed loop of the probes, typically water or water-glycol mixtures. Heat is



https://doi.org/10.52202/077185-0089

charged and discharged by heating or cooling the storage volume, and transported within the storage system exclusively by conduction, resulting in a more inert operational behavior compared to competing storage concepts. The need for peak load buffering by an additional buffer storage in the system is often the consequence (Fiorentini et al., 2023). In seasonal operation cycles involving charging the storage during summer months (April to September) and discharging during the heating season from October to March, it typically takes several years for these systems to level at a stable subsurface temperature and achieve maximum efficiency (Leitner, 2014).

The suitability of a site for BTES systems depends on the geological and hydrogeological characteristics of the immediate probe environment. Substrates with high heat capacity and density, such as water-saturated clay and rock layers, are advantageous (Nordell, 2016). The example shown in Table 1 illustrates that the total heat capacity of a storage with unfavorable geological conditions, such as dry gravel may be half that of a storage with favorable conditions, depending on the density and specific heat capacity (thermal properties by Nordell, 2016).

**Table 1:** Influence of storage medium properties on water equivalent (WE) storage volume

| **Storage medium** | **V_storage** m³ | **ρ_storage** kg/m³ | **$c_p$_storage** J/kgK | **ρ_water** kg/m³ | **$c_p$_water** J/kgK | **V_WE** m³ | **WE ratio** |
|---|---|---|---|---|---|---|---|
| Sandstone & molasse | 39000 | 2500 | 960 | 1000 | 4200 | 22286 | 1.75 |
| Gravel | 39000 | 1600 | 840 | 1000 | 4200 | 12480 | 3.13 |

This highlights the need for Thermal Response Tests in the planning process to access a reliable planning basis for each storage project. The metric "water equivalent" (WE) allows for comparison of different storage systems. The storage volume is converted to water-equivalent based on the specific heat capacity and density of the storage material (e.g. gravel), thereby representing the heat capacity equivalent to that of water in liquid state at normal pressure.

The system parameters of a BTES can be divided into the following categories: storage geometry, geological and hydrogeological conditions, and technical implementation. Table 2 shows a non-exclusive list of influencing parameters.

**Table 2:** BTES parameters

| **Category** | **Parameter** |
|---|---|
| Storage Geometry | probe length, probe spacing, probe arrangement, probe circuitry |
| Geological and Hydrogeological Conditions | Storage medium properties (water content, density, specific heat capacity) groundwater occurrence |
| Technical Implementation | probe type and dimensions, borehole diameter, borehole grouting conductivity, charge and discharge mass flows, storage inlet and outlet temperatures, probe fluid, insulation of top-layer |

To estimate the storage dimensions, the storage volume is determined based on the required amount of energy. Afterwards, the calculated values are verified against a BTES storage project in Crailsheim, Germany, and the procedure is repeated for a potential BTES for peak load coverage in Kempten. The storage volume is determined for a rectangular arrangement of probes with the probe length $L_{probe}$, spacing $S_{probe}$, and the number of probes $N_{probe}$, according to Equation 1.

$$V_{storage} = L_{probe} \cdot \left(S_{probe} \cdot \sqrt{N_{probe}}\right)^2 \tag{1}$$


https://doi.org/10.52202/077185-0089

With the average storage temperatures at the beginning ($T_1$) and end ($T_2$) of the charging and discharging periods, along with the volume-specific heat capacity of the soil $c_{ground,vol}$, the amount of heat stored in the BTES $Q_{storage}$ is calculated using the first law of thermodynamics, see Equation 2, and a volumetric heat capacity for the ground.

$$Q_{storage} = V_{storage} \cdot c_{ground,vol} \cdot (T_2 - T_1) \tag{2}$$

Table 3 shows the used parameters and results for the pre-dimensioning described in equations 1 and 2.

**Table 3:** Pre-dimensioning of BTES

| Symbol | Description | Crailsheim | Unit |
|---|---|---|---|
| | Probe arrangement | circular | |
| c_ground,vol | Spec. heat capacity ground (volumetric) | 2405 | kJ/(m³K) |
| S_probe | Probe center spacing | 3 | m |
| L_probe | Probe vertical length | 55 | m |
| n_probe | Number of probes | 80 | |
| V_storage | Effective volume of the storage | 37500 | m³ |
| T2 | Storage temperature charged | 53 | °C |
| T1 | Storage temperature discharged | 22 | °C |
| Q_storage | Usable thermal energy | 777 | MWh |
| η_storage | Estimated storage efficiency | 70 | % |
| Q_loss | Estimated storage losses | 333 | MWh |
| Q_charge | Estimated storage gross input | 1110 | MWh |

The determined amount of stored energy for Crailsheim, totaling 1110 MWh, corresponds approximately to the literature value of 1140 MWh (Bauer et al., 2007).

### 5.2 BTES Simulation Approach

In collaboration with Biberach University of Applied Sciences (HBC), a transient, semi-analytical storage model for BTES simulation based on g-functions and the superposition principle was developed using the established Eskilson model approach (Eskilson, 1987). In this process, Python code was integrated into a customizable component called MacroObject in the process simulation environment via a custom interface called EbsOpen module (Ebsilon, 2023).

The model incorporates the following features:

- Custom borefield characteristics using a custom g-function generator
- Dynamic calculation of borehole resistance using simplified model approaches according to Hellström
- Boundary condition for constant inlet temperature over equidistant time steps
- Calculation of, among other things, average borehole edge temperature, outlet temperature, specific extraction power per time step, pressure loss across the probe

Details of the developed model are provided in (Koenigsdorff, 2011; Eskilson, 1987; Miocic et al., 2024).

### 5.3 Case Study

The aim of the first case study of the BTES model is to demonstrate its functionality and compare the first results to the pre-dimensioning of the Crailsheim option shown in Table 3. All double-U probes are connected in parallel, and a continuous massflow per probe of 0.5 kg/s is chosen. During charge periods the probe inlet temperature is 60 °C and 20 °C during discharge, to achieve the average storage temperatures provided in Table 3. In Figure 3, the storage outlet temperature and the average borehole



https://doi.org/10.52202/077185-0089

edge temperature are plotted. It can be observed that in the last third of each discharge period, the difference between the borehole edge and fluid outlet temperatures significantly decreases.

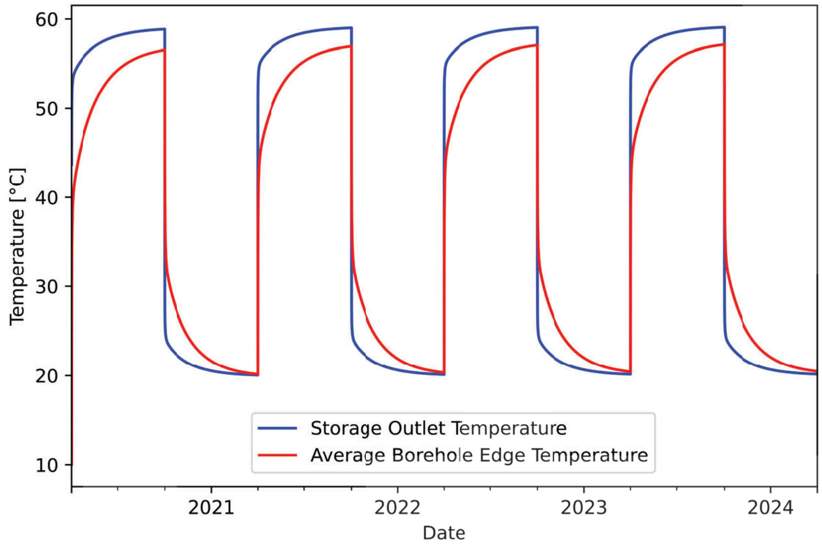


**Figure 3:** Crailsheim example: Storage temperature profiles over four years

Figure 4 illustrates the stored and discharged energy quantities. Compared to the pre-dimensioning shown in Table 3, slightly more heat is discharged (50-70 MWh). Approximately 300 MWh more heat is charged per period than assumed in the pre-calculation step. Therefore, the losses are higher compared to the estimated values (η_storage, Table 3). In the fifth year, it is approximately 10 %-points less efficient than assumed.

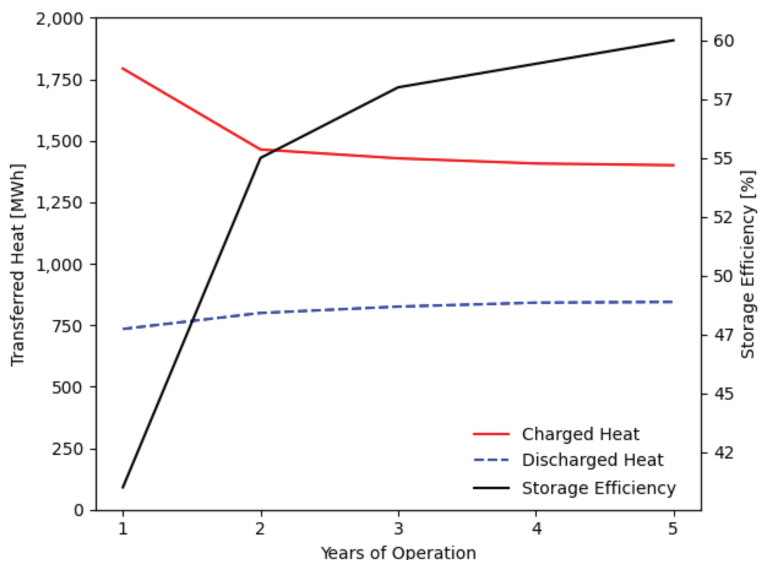


**Figure 4:** Comparison of charged and discharged heat over time

## 6 ECONOMIC ANALYSIS OF SELECTED SCENARIOS

An economic efficiency optimization is being performed for the ZAK heating network for a period of one year. The main scenario that is being investigated is to economically optimize peak load generation with the help of an additional large heat pump. The optimization is based on day-ahead exchange prices


https://doi.org/10.52202/077185-0089

for electricity and gas and the peak load profile of the district heating network described in chapter 3. Integrating the existing heat storage into the optimization makes it possible to increase the flexibility of the heat generation units. The optimized system with the additionally integrated heat pump is compared to the existing system.

The optimization is based on the DHC network peak load, as the waste incineration plant runs continuously throughout the year, covering the base load. For the heating network in question, the existing gas and oil burners of the peak load stations are simplified and assumed to be a single 45 $MW_h$ gas burner. To obtain a comparative value for the existing heating network and the optimized scenario, the following assumptions are made:

- Peak load boiler thermal output is adjustable between 0 % and 100 % with 95 % efficiency,
- Gas is procured via a day-ahead market,
- Investment and operating costs are taken from Table 4, and Table 5.

For the optimization, a 20 $MW_{th}$ heat pump is integrated into the district heating network. It is assumed that sufficient heat is available for the heat pump on the source side. A COP of 3 is selected based on the preliminary investigations (see chapter 5.3). The bandwidth of the output control of the heat pump is assumed to be in the range of 75 % - 100 %. The total costs $K^{total}$ calculated for the operating period of one year are based on the investment costs, the fixed operating costs and the variable operating costs. To calculate the investment costs, the maximum thermal output of the heat generator is multiplied by the specific investment costs. For the fixed operating costs, the maximum thermal output of the heat generator is multiplied by the specific fixed operating costs. The variable operating costs include the costs for gas procurement, a $CO_2$ tax and other variable operating costs for the gas boiler.

$$K^{total} = K^{invest} + K^{fix.operation} + K^{var.operation} \tag{3}$$

## 6.1 Optimization

A mixed-integer optimization is applied since binary variables are used to describe the state of the heat generators. The optimization is implemented in Python using the Pyomo package (Woodruff et al., 2021) and works with a solver from Gurobi (Gurobi Optimization 2024). In this case, the solver uses the simplex method to solve the optimization task.

## 6.2 Objective Function

The aim of the optimization is to minimize the variable operating costs for each time step t over one year (8760 h). For this purpose, the variable operating costs (K) of the respective heat generators are summed up, as shown in Equation 4. These are determined by the specific costs (k) multiplied by the power consumed. The power input is calculated using the COP or efficiency and the thermal power output, as shown in Equations 5 and 6.

$$min \sum_{t}^{8760} (K_t^{var.gas\,boiler} + K_t^{var.heat\,pump}) \tag{4}$$

$$K_t^{var.heat\,pump} = \frac{\dot{Q}_t^{hp}}{COP} \cdot (k_t^{elec} + k^{var.hp}) \tag{5}$$

$$K_t^{var.gas\,boiler} = \frac{\dot{Q}_t^{gas\,boiler}}{\eta_{gas}} \cdot (k_t^{gas} + k^{CO2} + k^{var.gas\,boiler}) \tag{6}$$

The peak load of the district heating network and the day-ahead prices for electricity and gas used in the optimization are from 2021. The assumptions for the grid utilization costs for electricity and gas are from 2023. They are shown in Table 4.



https://doi.org/10.52202/077185-0089

**Table 4:** Overview of grid utilization costs Germany (Bundesnetzagentur, 2023)

| | Electricity | Gas | Unit |
|---|---|---|---|
| Tax | 20.50 | 5.50 | €/MWh |
| Net. grid utilization | 33.00 | 3.90 | €/MWh |
| Measurement operation | 0.50 | 0.15 | €/MWh |
| Concession fee | 1.40 | 0.00 | €/MWh |
| Levys | 10.10 | - | €/MWh |
| $CO_2$ tax | - | 5.46 | €/MWh |
| **Sum** | **65.50** | **15.01** | **€/MWh** |

The procurement costs and grid utilization costs relate to Germany. The assumptions for operating and investment costs are shown in Table 5.

**Table 5:** Investment and operating costs (Danish Energy Agency, 2023)

| Investment costs | Heat pump (20 MW) | Gas boiler (10 MW) | Unit |
|---|---|---|---|
| Specific total | 1020 | 270 | k€/MW |
| Plant | 808 | 160 | k€/MW |
| Installation | 106 | 110 | k€/MW |
| Grid connection | 106 | - | k€/MW |
| **Operating costs** | | | |
| Service and maintenance | 3190.12 | 2658.43 | €/MW/a |
| Variable costs | 2.33 | 2.23 | €/MW |
| Electric cnergy | - | 0.11 | €/MW |
| Other var. costs | 2.33 | 2.12 | €/MW |

### 6.3 Optimization Results

Figure 5 shows the load distribution for a sample period with a high load on the left and a low load on the right.

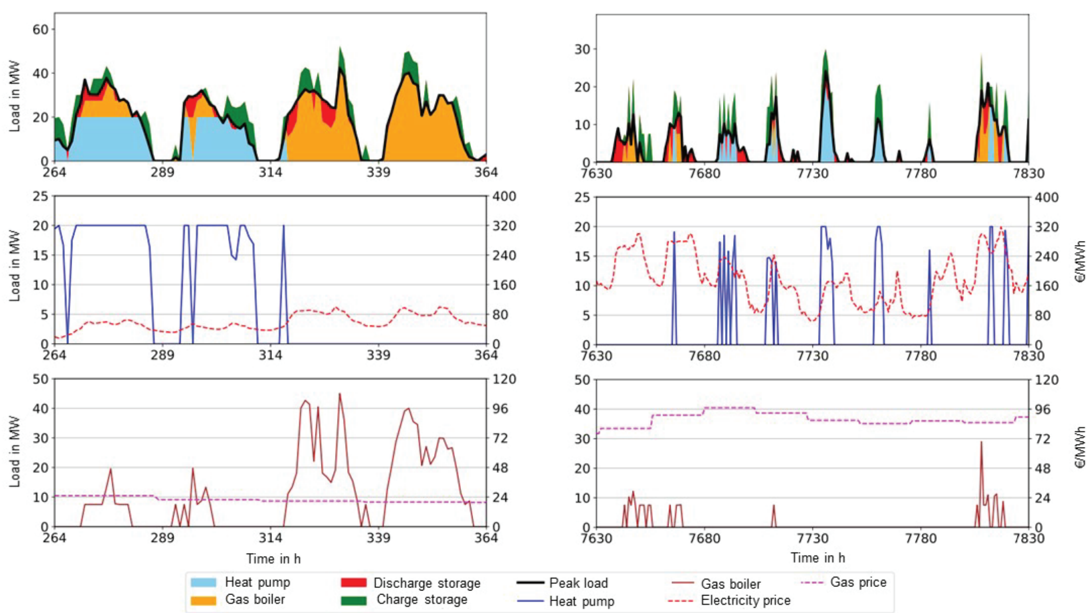


**Figure 5:** Load distribution optimization result for two selected timeframes


https://doi.org/10.52202/077185-0089

As shown on the left side, around 40 % of the load is covered by the heat pump. It can be seen how the heat pump is used at times of low electricity prices. As soon as electricity prices rise above a threshold of 80 €/MWh, it is no longer used and the peak load is covered by the gas boiler. During the period of low load, the heat pump not only covers the load but also fills the short-term heat storage. Even with a low load, there are times when operating the heat pump is more expensive than operating the gas boilers, and therefore the load is covered from the short-term heat storage or by the gas boilers.

Table 6 shows the total costs consisting of the investment costs, variable operating costs and fixed operating costs and calculates the savings for the optimized system as a percentage and an absolute value. The same is also calculated for the $CO_2$ emissions.

**Table 6:** Results of the optimization

| | **Initial system** | **Optimized system** | | |
|---|---|---|---|---|
| | Result in € | Result in € | Saving in € | Saving in % |
| Total cost | 14,615,186 | 22,605,542 | -7,990,3557 | - 54.67 |
| - Invest cost | 12,125,000 | 20,400,000 | -8,250,000 | -67.90 |
| - Var. operation cost | 2,345,556 | 2,022,111 | 323,445 | 13.79 |
| - Fix operation cost | 119,629 | 183,432 | - 63,802 | -53.33 |
| $CO_2$ emissions | 5,778 $tCO_2$ | 4,860 $tCO_2$ | 918 $tCO_2$ | 15.89 |

The investment costs in the existing system are only the costs for the gas boilers and the investment costs in the optimized system are only the cost for the large-scale heat pump. The total costs, calculated as in equation 4, are more than 50 % higher in the optimized system than for the existing system due to the significantly higher investment costs for the heat pump. In terms of variable operating costs, the optimization can achieve savings of around 14 %, which corresponds to 323,000 €. The fixed operating costs increase by around 53 % with the expansion of the heat pump. The reduction in the operating times of the gas boilers can also lead to a reduction in $CO_2$ emissions by around 918 $t_{CO2}$ compared to the existing system. In addition to the $CO_2$ emissions, the lower variable operating costs can also reduce the variable heating costs for the optimized year by 11 €/MWh.

### 6.4 Discussion

Table 6 shows that operating costs and the $CO_2$ emissions can be reduced by minimizing the operation of gas boilers using a large-scale heat pump. However, to achieve this, high investment costs for the large heat pump must be accepted.

Figure 5 showing the different load profiles indicates that the heat pump can be operated at times of low electricity prices and that the short-term heat storage is filled when the load is not completely covered. Increasing the capacity of the heat storage could improve the flexibility of the heat pump and thus further reduce the variable operating costs. The gas boilers cannot be completely replaced by the heat pump, as the output of the heat pump is not sufficient to completely cover the peak load of the district heating network.

## 7 CONCLUSIONS

In conclusion, the study has successfully developed models for high-temperature heat pumps and a comprehensive model for a Borehole Thermal Energy Storage. The models demonstrated that a system incorporating a large HTHP and a BTES can seasonally transfer a significant amount of excess heat. The economic analysis reveals that investing in a heat pump system remains economically viable, even with a conservative Coefficient of Performance (COP) of 3, given the high initial costs. However, it is crucial to acknowledge that the amortization of these costs occurs relatively late in the system's operational lifespan, underscoring the potential significance of grants or subsidies in supporting the economic viability of such systems.



https://doi.org/10.52202/077185-0089

Looking ahead, planned future research involves a more detailed economic analysis, incorporating the costs associated with energy storage solutions. The project extends its scope to investigate more applications that might be suitable for boosting the efficiency of DHC systems. Examples include excess heat utilization in the flue-gas scrubbing processes and mechanical vapor recompression (MVR) of low-pressure steam, the utilization of waste heat from carbon capture, hydrogen electrolysis, and battery storage power stations.

## ACKNOWLEDGEMENTS

This work was funded by the German Federal Ministry for Economic Affairs and Climate Action under the funding code 03EN3073, with additional financial and in-kind support from the project partners AGFW, Fernwärme Ulm GmbH, ZAK Energie GmbH, ecop Technologies GmbH and Siemens Energy GmbH & Co. KG. The responsibility for the content of this publication lies with the authors. The authors would like to thank Roland Koenigsdorff and Fabian Neth from Biberach University of Applied Sciences (HBC) and Nicole Negele from Kempten University of Applied Sciences for their cooperation and support during the study.

## NOMENCLATURE

| | | |
|---|---|---|
| ATES | Aquifer Thermal Energy Storage | (-) |
| BTES | borehole thermal energy storage | (-) |
| CHP | conventional heat pump | (-) |
| COP | coefficient of performance | (-) |
| DHC | district heating and cooling | (-) |
| RHP | rotation heat pump | (-) |
| WE | Water Equivalent | (-) |

**Symbols**

| | | |
|---|---|---|
| K | variable operating costs | (€) |
| k | specific costs | (€) |
| L | Length | (m) |
| N | Number | (-) |
| S | Spacing | (m) |

## REFERENCES

Ahrendts,Drechsler,Hendricks,Küpper,Lang,Peil,Scholz,Timofeeva, 2023. Roll-out of industrial heat pumps in Germany. https://doi.org/10.24406/publica-1440.

Arpagaus, C.,Bless, F.,Uhlmann, M.,Schiffmann, J.,Bertsch, S. S., 2018. High temperature heat pumps: Market overview, state of the art, research status, refrigerants, and application potentials. *Energy* 152, 985–1010.

Bauer,Heidemann,Müller-Steinhagen, 2007. Der Erdsonden-Wärmespeicher in Crailsheim.

Bolton, R.,Cameron, L.,Kerr, N.,Winskel, M.,Desguers, T., 2023. Seasonal thermal energy storage as a complementary technology. *Journal of Energy Storage* 73, 109249.

Bundesnetzagentur (Ed.), 2023. Monitoring Report 2023.

Danish Energy Agency (Ed.), 2023. Technology Data. Generation of Electricity and District Heating. 12th ed. Available online at https://ens.dk/sites/ens.dk/files/Analyser/version_12_-_technology_data_catalogue_for_el_and_dh.pdf (accessed 2/5/2024).

Dehli, M.,Doering, E.,Schedwill, H., 2023. Grundlagen der Technischen Thermodynamik. 10th ed. Wiesbaden, Springer Fachmedien Wiesbaden GmbH; Springer Vieweg.

Ebsilon, 2023. Iqony EBSILON. Available online at https://www.ebsilon.com/de/.



https://doi.org/10.52202/077185-0089

Eskilson, P., 1987. Thermal analysis of heat extraction boreholes. Available online at https://portal.research.lu.se/en/publications/thermal-analysis-of-heat-extraction-boreholes.

Federal Ministry for Economic Affairs and Climate Action (2024). The Heat Planning Act. Available online at https://www.bmwk-energiewende.de/EWD/Redaktion/EN/Newsletter/2023/11/Meldung/news1.html (accessed 2/19/2024).

Fiorentini, M.,Heer, P.,Baldini, L., 2023. Design optimization of a district heating and cooling system with a borehole seasonal thermal energy storage. *Energy* 262, 125464.

Fleuchaus, P., 2020. Global application, performance and risk analysis of ATES. https://doi.org/10.5445/IR/1000120042.

Gurobi Optimization (2024). The Leader in Decision Intelligence Technology. Available online at https://www.gurobi.com/ (accessed 2/23/2024).

Hirvijoki, E.,Hirvonen, J., 2022. The potential of intermediate-to-deep geothermal boreholes for seasonal storage of district heat. *Renewable Energy* 198, 825–832.

Jiang, J.,Hu, B.,Wang, R. Z.,Liu, H.,Zhang, Z.,Li, H., 2021. Theoretical performance assessment of low-GWP refrigerant R1233zd(E) applied in high temperature heat pump system. *International Journal of Refrigeration* 131, 897–908.

Koenigsdorff, R., 2011. Oberflächennahe Geothermie für Gebäude. Grundlagen und Anwendungen zukunftsfähiger Heizung und Kühlung. Stuttgart, Fraunhofer IRB Verlag.

Längauer, A., 2021. Vergleich der Rotationswärmepumpe mit konventionellen Kompressionswärmepumpen in industriellen Prozessen. ecop Technologies GmbH; OST – Ostschweizer Fachhochschule, Institut für Energiesysteme. Available online at https://www.ecop.at/wp-content/uploads/2022/01/2021-DKV_AA_IV_21_L%C3%A4ngauer.pdf (accessed 2/19/2024).

Längauer, A.,Adler, B. The Joule cycle realised in a rotation heat pump. *14th IIR-Gustav Lorentzen Conference on Natural Refrigerants (GL2020). Proceedings. Kyoto, Japan*.

Längauer, A.,Adler, B.,Rakusch,et al., 2019. COP tests of a rotation heat pump. *Proceedings of the 25th IIR International Congress of Refrigeration: Montréal, Canada*.

Leitner, S., 2014. Physik neuartiger Wärmespeicher. Hamburg, diplom.de.

Miocic, J. M.,Schleichert, L.,van de Ven, A.,Koenigsdorff, R., 2024. Fast calculation of the technical shallow geothermal energy potential of large areas with a steady-state solution of the finite line source. *Geothermics* 116, 102851.

Nickel, M., 2023. Die Energieversorgung 2023 - Jahresbericht. BDEW e.V. Available online at https://www.bdew.de/media/documents/Jahresbericht_2023_Foliensatz_final_18Dez2023_V2.pdf (accessed 2/19/2024).

Nordell, B., 2016. Borehole heat store design optimization. Luleå tekniska universitet. https://doi.org/999609.

Pelda, J.,Stelter, F.,Holler, S., 2020. Potential of integrating industrial waste heat and solar thermal energy into district heating networks in Germany. *Energy* 203, 117812.

Technology Collaboration Programme on Heat Pumping Technologies by IEA (Ed.), 2022. Industrial Heat Pump Annex 58.

Welsch, B.,Rühaak, W.,Schulte, D. O.,Bär, K.,Sass, I., 2016. Characteristics of medium deep borehole thermal energy storage. *International Journal of Energy Research* 40 (13), 1855.

Woodruff, D. L.,Watson, J.-P.,Siirola, J. D.,Nicholson, B. L.,Laird, C. D.,Hart, W. E.,Hackebeil, G. A.,Bynum, M. L., 2021. Pyomo Optimization Modeling in Python. Cham, Springer.



https://doi.org/10.52202/077185-0089